Polyoxometalate-supported ruthenium nanoparticles as bifunctional heterogeneous catalysts for the conversions of cellobiose and cellulose into sorbitol under mild conditions

Mi Liu, Weiping Deng, Qinghong Zhang,* Yanliang Wang and Ye Wang*

State Key Laboratory of Physical Chemistry of Solid Surfaces, National Engineering Laboratory for Green Chemical Productions of Alcohols, Ethers and Esters, College of Chemistry and Chemical Engineering, Xiamen University, Xiamen 361005, China

Electronic Supplementary Information

1. Experimental details

(1) Catalyst preparation

The Cs salts of tungstophophates with different Cs contents ($Cs_xH_{3-x}PW_{12}O_{40}$, $x = 1.0$-3.0) were prepared by a reaction between $H_3PW_{12}O_{40}$ and Cs_2CO_3. The precipitates obtained after the addition of the aqueous solution of Cs_2CO_3 into that of $H_3PW_{12}O_{40}$ were recovered by filtration, followed by washing with water, drying and calcination at 673 K for 2 h to obtain the $Cs_xH_{3-x}PW_{12}O_{40}$ samples.

The $Ru/Cs_xH_{3-x}PW_{12}O_{40}$ catalysts were prepared by an adsorption of colloidal Ru nanoparticles onto the $Cs_xH_{3-x}PW_{12}O_{40}$. Colloidal Ru nanoparticles with a mean size of 1.6 nm were preliminarily prepared by the reduction of $RuCl_3$ with ascorbic acid at 353 K. The typical TEM micrograph and the particle size distribution of the colloidal Ru nanoparticles prepared above are shown in Fig. S1. Then, the $Cs_xH_{3-x}PW_{12}O_{40}$ white powders were added into the aqueous solution containing these colloidal Ru nanoparticles. The addition of the polyoxometalate powders decoloured the solution, while the colour of the support was deepened, indicating the adsorption of Ru nanoparticles onto the support. After filtration, washing with deionised water and drying at 373 K, the $Ru/Cs_xH_{3-x}PW_{12}O_{40}$ catalysts were obtained. The same procedure was also employed for the preparation of Ru nanoparticles loaded on other acidic solid supports. The loading of Ru was kept at 1.0 wt% in each catalyst.

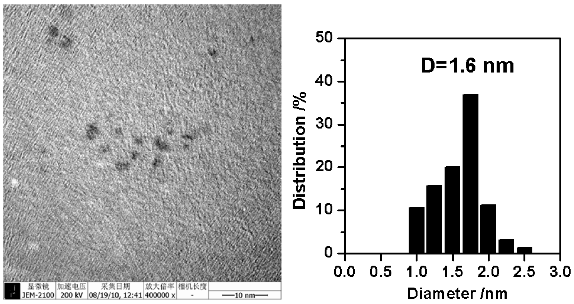

Fig. S1 TEM micrograph and particle size distribution of colloidal Ru nanoparticles.

(2) Catalyst characterization

The catalysts were characterized by Powder X-ray diffraction (XRD), N_2 physisorption, CO chemisorption, transmission electron microscopy (TEM), NH_3-temperature-programmed desorption (NH_3-TPD) and pyridine-adsorbed Fourier-transform infrared (FT-IR) spectroscopic techniques.

XRD patterns were collected on a Panalytical X'pert Pro diffractometer using Cu K_{α} radiation (40 kV, 30 mA). The Keggin structure of $Cs_xH_{3-x}PW_{12}O_{40}$ was confirmed by XRD measuremments.

N_2 physisorption was carried out with a Micromeritics Tristar 3000 surface area and porosimetry analyzer to examine the surface area and porous structure of the catalyst. The surface areas of the 1 wt% Ru/ $Cs_xH_{3-x}PW_{12}O_{40}$ with x values of 1.0, 1.5, 2.0, 2.5 and 3.0 were 59, 60, 76, 93 and 98 m^2 g^{-1}, respectively.

Ru dispersions were measured by CO chemisorption using an ASAP2010C Micromeritics apparatus. The Ru dispersion for the 1 wt% $Ru/Cs_3PW_{12}O_{40}$ was 0.487, corresponding to a size of Ru particle of 1.9 nm, which was close to the mean size of the precursor of collodal Ru nanoparticles (1.6 nm, Fig. S1).

TEM measurements were performed on a JEM-2100 electron microscope operated at an acceleration voltage of 200 kV.

NH_3-TPD was performed on a Micromeritics AutoChem 2920 II instrument. Typically, the sample loaded in a quartz reactor was first pretreated with high-purity He at 573 K for 1 h. After the sample was cooled to 373 K, NH_3 adsorption was performed by switching the He flow to a NH_3-He (10 vol% NH_3) gas mixture and then keeping at 373 K for 1 h. Then, the gas phase or the weakly adsorbed NH_3 was purged by high-purity He at the same temperature. NH_3-TPD was performed in the He flow by raising the temperature to 1073 K at a rate of 10 K min^{-1}, and the desorbed NH_3 molecules were detected by ThermoStar GSD 301 T2 mass spectrometer with the signal of $m/e = 16$.

Pyridine-adsorbed FT-IR was performed with a Nicolet Avatar 330 instrument equipped with an MCT detector with a resolution of 4 cm^{-1}. The sample was pressed into a self-supported wafer, and placed in an in situ IR cell. After pretreatment in H_2 at 573 K, followed by evacuation at the same temperature, the sample was cooled down to 423 K and was exposed to pyridine for 0.5 h. After cooling down to 303 K under vacuum, H_2 was introduced. FT-IR spectra were recorded under H_2 with different pressures and at 303 or 323 K.

(3) Catalytic reactions

The conversion of cellobiose or cellulose was performed with a batch-type high-pressure autoclave reactor. Typically, the catalyst (0.10 g) and cellobiose (0.20 g) were added into a

Teflon-lined stainless-steel reactor pre-charged with H_2O (10 cm^3), and then the reaction was carried out at 413 K under 2 MPa H_2 for 6 h. After the reaction, the solid catalyst was separated by centrifugation, and the liquid products were analyzed by a HPLC (Shimazu LC-20A) equipped with a RI detector and a Transgenomic^{TM} CARBONSep CHO-620 column (10 μm, 6.5×300 mm). The eluent was water with a flow rate of 0.5 cm^3 min^{-1}. The column was thermostated at 338 K by a column heater. Sampling loop has a volume of 20 μL. For the conversion of cellulose, microcrystalline cellulose purchased from Alfa Aesar with a crystallinity of 85% was ball-milled before use.

2. Structural formulas of reactants and products

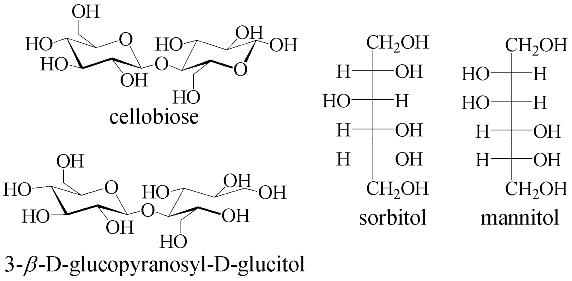

Scheme S1 Structural formulas of reactants (cellobiose) and products (3-β-glucopyranosyl-D-glucitol, sorbitol and mannitol).

3. NH_3-TPD profiles for some typical solid acid materials used in this work

Fig. S2 shows the NH_3-TPD profiles for some typical solid acid materials used in this work. From the NH_3 desorption peak, it is clear $Cs_{2.0}H_{1.0}PW_{12}O_{40}$ possesses stronger acidity than H-ZSM-5 and MCM-22, while $Cs_{3.0}PW_{12}O_{40}$ does not possess any acidity.

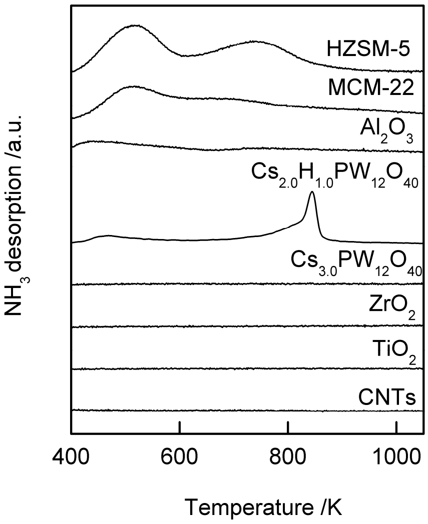

Fig. S2 NH_3-TPD profiles for some typical solid acid materials used in this work.

4. Catalytic performances of the Ru/$Cs_xH_{3-x}PW_{12}O_{40}$ with different Cs contents for the conversion of cellobiose into sorbitol

Table S1 shows the catalytic performances of the 1.0 wt% Ru/$Cs_xH_{3-x}PW_{12}O_{40}$ with different Cs contents for the conversion of cellobiose into sorbitol in water in H_2.

Table S1 Catalytic performances of the 1.0 wt% Ru/$Cs_xH_{3-x}PW_{12}O_{40}$ with different Cs contents for the conversion of cellobiose into sorbitol in water in H_2[a]

Catalyst	Conversion (%)	Yield (%)		
		glucose	sorbitol	3-β-glucopyranosyl-D-glucitol
1 wt% Ru/$Cs_{1.0}H_{2.0}PW_{12}O_{40}$	100	0.9	94	-
1 wt% Ru/$Cs_{1.5}H_{1.5}PW_{12}O_{40}$	100	1.6	92	1.1
1 wt% Ru/$Cs_{2.0}H_{1.0}PW_{12}O_{40}$	100	1.2	93	1.2
1 wt% Ru/$Cs_{2.5}H_{0.5}PW_{12}O_{40}$	100	1.1	93	0.7
1 wt% Ru/$Cs_{3.0}PW_{12}O_{40}$	100	2.3	86	11

[a] Reaction conditions: catalyst, 0.10 g; cellobiose 0.058 mol dm^{-3}; water, 10 cm^3; H_2, 2 MPa; temperature, 413 K; time, 6 h.

5. Pyridine-adsorbed FT-IR spectra for the Ru/$Cs_3PW_{12}O_{40}$ and Ru/$Cs_2HPW_{12}O_{40}$ catalysts before and after repeated uses

The Ru/$Cs_3PW_{12}O_{40}$ and Ru/$Cs_2HPW_{12}O_{40}$ catalysts before and after cellobiose conversions under the conditions of Fig. 2 were pretreated at 573 K under vacuum for 0.5 h to remove physical adsorbed water, and then were cooled down to 423 K and exposed to pyridine for 0.5 h. The FT-IR spectra were recorded after evacuation at 423 K for 0.2 h. Fig. S3 shows that the fresh Ru/$Cs_2HPW_{12}O_{40}$ catalyst exhibits a strong IR band at 1540 cm^{-1}, which is ascribed to pyridine adsorbed on the Brønsted acid sites (Fig. S3, curve b). However, the intensity of this IR band decreased significantly for the same catalyst after repeated reactions (Fig. S3, curve d), suggesting the leaching of protons from the Ru/$Cs_2HPW_{12}O_{40}$ catalyst. On the other hand, for the Ru/$Cs_3PW_{12}O_{40}$ catalyst, the IR band ascribed to Brønsted acid was not observed before reaction (Fig. S3, curve a), consistent with the fact that no intrinsic Brønsted acid sites existed on this catalyst. However, a weak IR band at 1540 cm^{-1} appeared over the Ru/$Cs_3PW_{12}O_{40}$ catalyst after the repeated reactions in H_2 (Fig. S3, curve c), suggesting the generation of a small amount of Brønsted acid sites over this catalyst. We believed that these Brønsted acid sites were originated from H_2. Thus, although the acidities of the fresh Ru/$Cs_2HPW_{12}O_{40}$ and Ru/$Cs_3PW_{12}O_{40}$ catalysts were quite different, these catalysts after reactions showed similar acidities (Fig. S3, curves c and d).

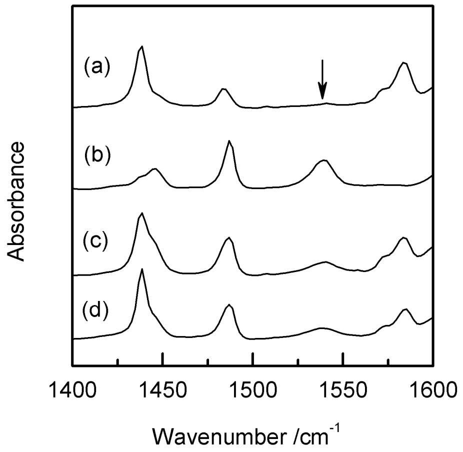

Fig. S3 Pyridine-adsorbed FT-IR spectra for the Ru/$Cs_3PW_{12}O_{40}$ and Ru/$Cs_2HPW_{12}O_{40}$ before and after reactions followed by evacuation at 423 K. (a) Ru/$Cs_3PW_{12}O_{40}$ before reaction, (b) Ru/$Cs_2HPW_{12}O_{40}$ before reaction, (c) Ru/$Cs_3PW_{12}O_{40}$ after reaction, (d) Ru/$Cs_2HPW_{12}O_{40}$ after reaction.

6. Effect of Ru loadings on catalytic performances of the Ru/$Cs_3PW_{12}O_{40}$ catalysts for the conversion of cellobiose into sorbitol

Fig. S4 shows the catalytic performances of the Ru/$Cs_3PW_{12}O_{40}$ catalysts with different Ru loadings for the conversion of cellobiose into sorbitol in water in H_2. Without Ru, cellobiose conversion was quite low, and the main product was glucose. The increase in Ru loadings up to 0.5 wt% significant increased cellobiose conversion. Sorbitol yield increased also after the loading of Ru. It is notable that glucose yield also increased after the loading of a small amount of Ru. We believe that, the dissociation of H_2 on Ru nanoparticles to H species, which can spillover to $Cs_3PW_{12}O_{40}$ surfaces, causes the generation of the Brønsted acidic sites.

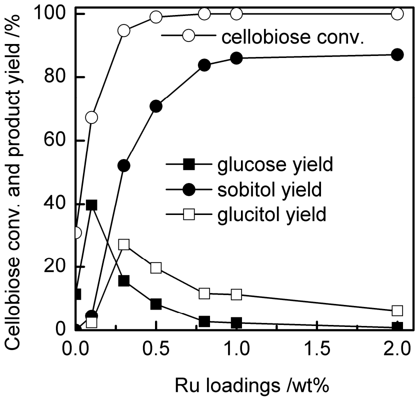

Fig. S4 Catalytic performances of the Ru/$Cs_3PW_{12}O_{40}$ catalysts with different Ru loadings for the conversion of cellobiose into sorbitol in water in H_2. Reaction conditions: catalyst, 0.10 g; temperature, 413 K; cellobiose, 0.058 mol dm^{-3}; water, 10 cm^3; H_2, 2 MPa; time, 6 h.

7. Pyridine-adsorbed FT-IR spectra for the Ru/Al_2O_3 catalyst in H_2 with different pressures

Fig. S5 shows the pyridine-adsorbed FT-IR spectra for the Ru/Al_2O_3 catalyst in H_2 with different pressures. The same experimental procedures were adopted with those for the Ru/$Cs_3PW_{12}O_{40}$ catalyst. The IR band ascribed to pyridine adsorbed on Brønsted acid sites at 1540 cm^{-1} could not be observed even after the introduction of H_2 with a pressure of 44.8 kPa at 323 K (Fig. S5, curves b-f). This indicates that the generation of Brønsted acid sites from spillover hydrogen over the Ru/Al_2O_3 catalyst is not easy under the conditions used for the Ru/$Cs_3PW_{12}O_{40}$.

In our previous work, we have already demonstrated that the production of sorbitol from cellobiose requires not only hydrogenation of glucose moiety but also hydrolysis of the glycosidic bond.[1] It can be expected that the Brønsted acid sites account for the hydrolysis step, while the Ru nanoparticles are responsible for hydrogenation. Because the Ru/Al_2O_3 catalyst could not generate the Brønsted acid sites in H_2, it is understandable that it only showed a quite low yield of sorbitol. The reason for the low yields of sorbitol over Ru catalysts on some other supports such as TiO_2, ZrO_2, MCM-22 and CNT might be the same as that for the Ru/Al_2O_3 catalyst.

For the Ru catalyst supported on H-ZSM-5, which possesses Brønsted acid sites in the micropores, the low yield of sorbitol may result from the limit of the micropore size. It is reported that one glucose molecule is ~0.5 nm in diameter.[2] Therefore, it is not easy for cellobiose to enter the micropore of H-ZSM-5 (pore diameter, ~0.55 nm).

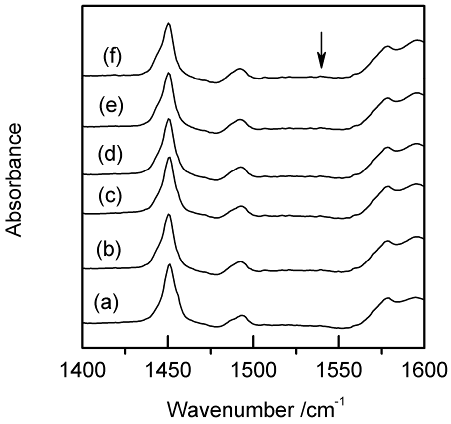

Fig. S5 Pyridine-adsorbed FT-IR spectra for the Ru/Al_2O_3 in H_2 with different pressures at 303 K or 323 K. (a) after pretreatment in H_2 at 573 K followed by evacuation, (b) 12.8 kPa H_2 and 303 K, (c) 19.2 kPa H_2 and 323 K, (d) 25.6 kPa H_2 and 323 K, (e) 33.3 kPa H_2 and 323 K, (f) 44.8 kPa H_2 and 323 K.

8. Catalytic performances of the Ru/$Cs_3PW_{12}O_{40}$ catalyst with and without H_2 pretreatment for the hydrolysis of cellulose in N_2 atmosphere

Table S2 shows the catalytic performances of the Ru/$Cs_3PW_{12}O_{40}$ catalysts with and without H2 pretreatment. The catalyst after pretreatment in H_2 at 573 K for 5 h was denoted as

Ru/$Cs_3PW_{12}O_{40}$ (H-5). Table S2 shows that the hydrolysis of cellulose in N_2 over the Ru/$Cs_3PW_{12}O_{40}$ catalyst mainly produces glucose, fructose and cellobiose, but their yields were very low as compared the yields of products obtained from the conversion of cellulose in H_2 (sorbitol, ~40%). Moreover, the pretreatment of the Ru/$Cs_3PW_{12}O_{40}$ catalyst by H_2 at 573 K did not exert significant positive effects on the yields of hydrolysis products. This further suggests the key role of the presence of H_2 in the conversion of cellulose.

Table S2 Catalytic performances of the 1.0 wt% Ru/$Cs_3PW_{12}O_{40}$ and 1.0 wt% Ru/$Cs_2HPW_{12}O_{40}$ for the conversion of cellulose into glucose in water in N_2[a]

Catalyst	Yield (%)		
	Glucose	Fructose	Cellobiose
1 wt% Ru/$Cs_3PW_{12}O_{40}$	4.2	1.3	0.8
1 wt% Ru/$Cs_3PW_{12}O_{40}$ (H-5)	4.8	1.2	0.8

[a] Reaction conditions: catalyst, 0.10 g; cellulose 0.10 g; water, 15 cm^3; N_2, 2 MPa; temperature, 433 K; time, 24 h.

References

1. W. Deng, M. Liu, X. Tan, Q. Zhang and Y. Wang, *J. Catal.*, 2010, **271**, 22-32.
2. R. Rinaldi and F. Schüth, *Energy Environ. Sci.*, 2009, **2**, 610-626.